JOURNAL OF MATERIALS SCIENCE 13 (1978) 2003–2012

Strength improvement of cemented carbides by hot isostatic pressing (HIP)

ULF ENGEL, HEINZ HÜBNER
Institut für Werkstoffwissenschaften, University of Erlangen-Nürnberg, 8520 Erlangen, Martensstrasse 5, Germany

HIP treatment after sintering increases the strength of the investigated cemented carbide alloy by a factor of two whereas hardness, fracture toughness, and work of fracture remain unchanged. HIP does not affect the microstructural parameters of the carbide skeleton and the binder phase, but the residual pores are eliminated entirely. Failure of both the as-sintered and post-densified material occurs by a pure Griffith mechanism. The strength–flaw size relationship is established experimentally and is shown to obey exactly Griffith's basic strength equation. The strength is controlled by the largest microstructural defects, i.e. pores in the as-sintered material, and coarse WC grains and inclusions in the HIP-treated specimens.

Nomenclature

a size of the fracture initiating flaw
a_{th} theoretical flaw size
b sample thickness
c length of the pre-crack
C contiguity of the carbide phase
$\bar{D}_{WC}$ mean carbide grain size
E Young's modulus
F fracture surface
G_{IC} critical energy release rate
h sample height
H_V Vicker's hardness
K_{IC} critical stress intensity factor
l span length
l_{Co} mean Co layer thickness
m Weibull parameter
P load
r_{pl} radius of the plastic zone
R crack resistance
S probability of failure
U fracture energy
X relative crack length
Y K-calibration
γ_F specific work of fracture
γ_I specific energy for fracture initiation
ϵ spread of grain size distribution
λ compliance of the pre-cracked specimen
λ_0 compliance of the uncracked specimen
ν Poisson's ratio
σ fracture stress
σ_0 maximum stress
σ_B bend strength
σ_Y Yield strength
σ_{eff} maximum local stress

1. The strength of cemented carbides

Attempts to improve the strength of cemented carbides by a reduction of the porosity have been reported by several authors (for example, Anderson [1] and Suzuki and Hayashi [2]). All these investigations emphasize the necessity to keep the porosity as low as possible. However, this condition can only be satisfied up to a certain limit because a small amount of residual porosity always remains when the material is fabricated by normal or even by optimized sintering. Using the HIP treatment as an additional fabrication process, however, the residual porosity can be eliminated almost entirely, considerably influencing the strength of the alloys. An improvement in strength up to 70% due to HIP has been reported by Lardner and Bettle [3] and by Rüdiger and Exner [4].

Cemented carbides are widely known to represent a group of very brittle materials. Thus, their mechanical behaviour should be explicable

in terms of Griffith's theory of brittle fracture rather than by theories which describe the failure of high-strength materials in terms of some limited amount of ductility. The Griffith equation as modified by Davidge and Evans [5]

$$\sigma_B = \frac{1}{Y}\left(\frac{2\gamma_I E}{a(1-\nu^2)}\right)^{1/2} \quad (1)$$

states that the bend strength of a brittle material, σ_B, is determined by two fundamental parameters. These are the size of the fracture-initiating flaws, a, and the amount of the specific energy for fracture initiation, γ_I. γ_I is related to the critical stress intensity factor of the material, K_{IC}, by the Irwin equation

$$K_{IC}^2 = 2\gamma_I E/(1-\nu^2). \quad (2)$$

Both γ_I and K_{IC} are material parameters which have an identical meaning. They define the "bulk strength" of a brittle material without flaws. Using Equation 2, Equation 1 may be written as

$$\sigma_B = \frac{1}{Y}\frac{K_{IC}}{a^{1/2}}. \quad (3)$$

Equation 3 states that the strength of a brittle material can be improved either if K_{IC} is increased or if the flaw size is decreased. If that approach (originally derived by Griffith for glass materials) can also be applied to cemented carbides, the strength increase due to HIP can easily be understood as a consequence of the reduction of the porosity. On the other hand, however, it is conceivable that during the HIP treatment metallurgical processes, like the formation of precipitates, can occur both in the binder metal and in the carbide phase or even between them which possibly cause a K_{IC} increase. The dependence of the HIP effect on the temperature as well as on the composition of the cemented carbide alloy [4] may be indicative for such kind of transformations. No investigations have been published up till now to determine which of the above two mechanisms is responsible for the increase in strength of cemented carbides by HIP, and neither has any attempt been made to interpret the mechanical behaviour of these alloys, on the whole, in terms of Griffith's theory. Nevertheless, the HIP effect on the strength is considered in the literature to be caused by the flaw-size reduction only.

It was the aim of this work to find a theoretical approach to the strength and fracture behaviour of cemented carbides on the basis of fracture mechanics and Griffith's theory which could be verified experimentally by a correlation of the macroscopic strength data with microstructural parameters. For this purpose a series of microstructural and mechanical data has been determined on three grades of the same basic material which differed in thermal treatment (as-sintered, HIP-treated below and above the temperature of the WC–Co eutectic).

Some efforts have been made in this work to determine the K_{IC} value correctly because it represents a material property which is very sensitive to the way of notching or pre-cracking. Former studies on K_{IC}-testing of cemented carbides as published [6–11] have shown that depending on the sample type, sample dimensions, notch depth, and notch geometry a wide spread of inconsistent results can be achieved. A summary of previous work on the measurement of K_{IC} of cemented carbides has been given recently by Hübner and Engel [12]. To make sure that the alterations in K_{IC} as caused by the HIP process are not concealed by such erroneous influences, the validity of the K_{IC} determination method was proved carefully. An additional means to confirm the validity of K_{IC} results was found in the determination of the crack resistance curve.

2. Experimental technique and evaluation method

2.1. Materials

The investigations were carried out on a test alloy supplied by Friedr. Krupp GmbH, Forschungsinstitut, Essen, which had been fabricated particularly for test purposes. The composition of the alloy was 92 wt % WC, 2 wt % TaC, and 6 wt % Co. Starting from this base material two additional variations were produced by different HIP treatments resulting in three grades of the same alloy:

Grade A; as-sintered

Grade B; isostatically densified by HIP (1260° C, 1 h, 1 kbar)

Grade C; isostatically densified by HIP (1360° C, 1 h, 1 kbar).

2.2. Measured parameters

To obtain a comprehensive survey on the properties affected by HIP a large range of experimental data was measured. These are:

(*a*) microstructural parameters (mean grain size of the carbide phase, mean Co layer thickness, and contiguity, using the quantitative analysis given by Exner [13, 14],

(*b*) change in porosity (optical microscopy and precision density measurements),

(*c*) Young's modulus (dynamic method)

(*d*) Vicker's hardness (H_V 20)

(*e*) bend strength (according to ISO standard 3327)

(*f*) specific work of fracture and

(*g*) critical stress intensity factor.

The size of the fracture-initiating flaws was determined using scanning electron microscopy (SEM).

2.3. Work of fracture

The specific work of fracture γ_F is a quantitative measure of the energies consumed during crack propagation. It can be determined in a bend test using Nakayama's technique [15] of controlled fracture. According to [11] this technique can also be applied to cemented carbide materials provided the samples contain a triangular notch as proposed by Tattersall and Tappin [16], Fig. 1. If the cracking occurs in a completely controlled way the value of γ_F is determined from the area under the load–deflection curve.

$$\gamma_F = U/2F. \tag{4}$$

A record of a controlled fracture experiment on a cemented carbide bend specimen is given in Fig. 1.

2.4. Determination of the fracture toughness

A comparison of previous studies on fracture toughness testing of cemented carbides [12] has shown that only samples containing sharp cracks can be used to obtain valid K_{IC} measurements This fact is in contrast to fracture mechanics testing of ceramic materials of comparable brittleness where sawn notches are employed frequently. In this work, sharp cracks were introduced into bend specimens by applying once again the technique of controlled fracture experiments. This method has been suggested by Hübner and Jillek [17] who produced natural cracks of any desired length in bend specimens of alumina. In a controlled fracture experiment a steady amount of energy must be supplied to the specimen to keep the crack moving. Thus, the crack propagation can be arrested at any position along the falling part of the load–deflection curve by stopping the testing machine. The pre-cracked sample is then subjected to a subsequent K_{IC} test [17].

In considering pre-cracks in cemented carbide materials it seemed that the Tattersall–Tappin notch had to be placed very deep into the specimen cross-section in order to obtain controlled fracture. For that reason through cracks could only be achieved at relative crack length values in the range $0.75 < X < 0.80$. Details on cemented carbide pre-cracking are reported in [12].

Because of the large length of the pre-cracks and the small specimen dimensions two problems arose in calculating the fracture toughness value from the basic equation

$$K_{IC} = \sigma_0 Y\sqrt{c}. \tag{5}$$

Firstly, it was difficult to measure the crack length in the opaque material with sufficient accuracy. Secondly, for crack lengths where $X > 0.75$, in the K-calibration Y is strongly dependent on X so that

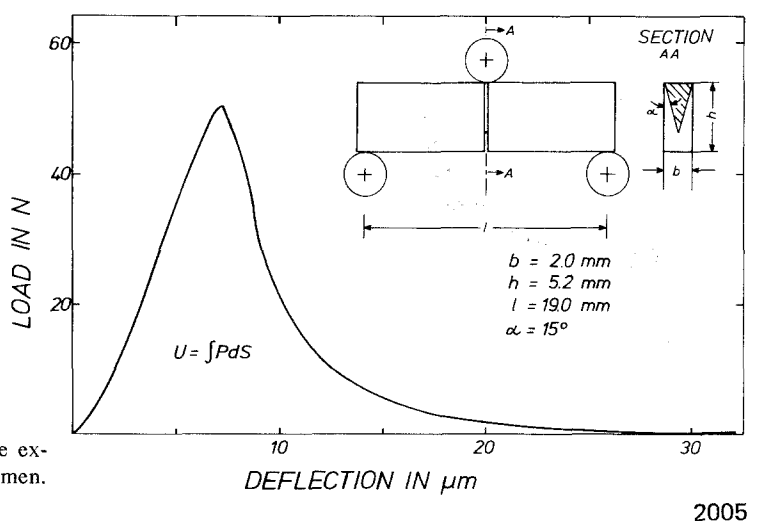

Figure 1 Plot of a controlled fracture experiment on a cemented carbide specimen.

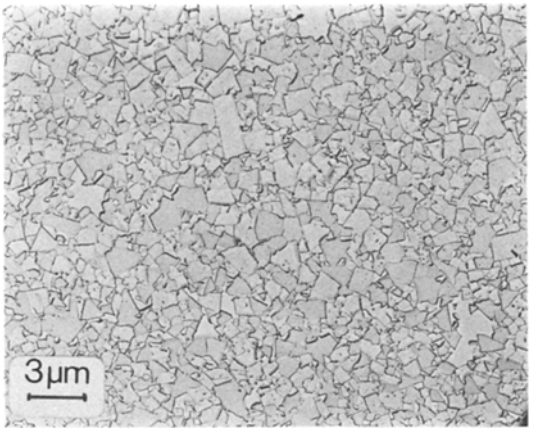

Figure 2 Microstructure of the test material (TEM replica technique).

even a small experimental error in X causes a large deviation in Y. Both difficulties were circumvented using another formula for K_{IC} instead of Equation 5 which had been derived to replace c and Y by a function of the specimen compliance, λ.

$$K_{IC} = C_1 \frac{Pl}{bh^{3/2}} \left(\frac{l}{9h(1-\nu^2)} \frac{\lambda - \lambda_0}{\lambda_0} - C_2 \right)^{3/4} \quad (6)$$

where C_1 and C_2 are numerical constants. The derivation of Equation 6 is given in [12].

To obtain K_{IC} from Equation 6 the maximum load at failure and the compliance of the precracked specimen must be known. The crack length, however, need not be determined. Both P and λ can be obtained easily from the load-deflection record of the K_{IC} test with great accuracy.

Figure 3 Characteristic types of microstructural inhomogeneities; (a) large pore in Grade A material, (b) Co pool in Grade B material, and (c) coarse WC grain in Grade C material.

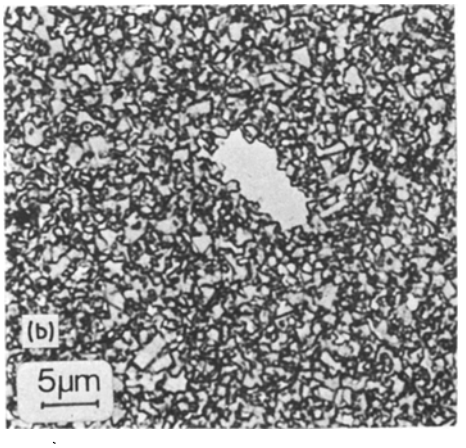

TABLE I Microstructural parameters

Grade	$\bar{D}_{WC}$ (μm)	ϵ	l_{Co} (μm)	C
A	0.76	0.34	0.20	0.58
B	0.75	0.40	0.21	0.59
C	0.77	0.36	0.21	0.58

3. Results

3.1. Microstructure

The microstructure of the test material is shown in Fig. 2. To achieve a high resolution, the TEM replica technique was used. A quantitative metallographic analysis [13, 14] was made to obtain the microstructural parameters listed in Table I. The cemented carbide material is characterized by a small Co-layer thickness, a great contiguity of the carbide phase, and a very small carbide grain size which obeys a log–normal size distribution. The main result of Table I is the fact that the

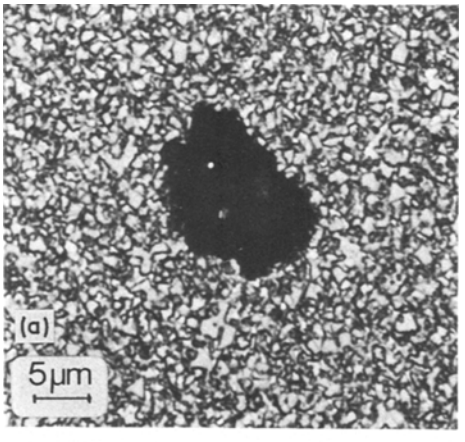

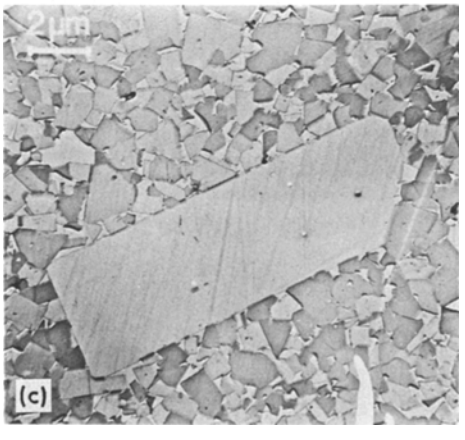

TABLE II Mechanical properties

Grade	E (GN m^{-2})	σ_B (MN m^{-2})	m	H_V20	γ_F	γ_I	K_{IC} (MN m$^{3/2}$)
A	623.6	1240	8.4	16.7	68.6	58.6	8.96 ± 0.25
B	623.6	2540	8.8	16.7	69.2	59.0	8.99 ± 0.14
C	623.6	2330	14.8	16.6	71.0	55.0	8.68. ± 0.22

microstructural data of Grade B and C materials are essentially not altered by the HIP treatment.

There are characteristic types of inhomogeneities present in each grade of the material which is obviously due to the different heat treatment. These features are shown in Fig. 3. In Grade A, pores of about 20 to 50 μm in diameter prevail (Fig. 3a). These pores are completely eliminated in Grades B and C. The reduction of porosity is also observed in precision density measurements which reveal an increase in density of 0.16% in both Grades B and C. The material of Grade B shows Co pools (Fig. 3b) which are supposed to be created by the plastic flow of the binder metal into the former pores. The size distribution of the Co pools, however, is only 5 to 10 μm. This indicates that the WC skeleton must have been deformed as well during the HIP treatment. Even these pools are absent in samples of Grade C. Because of the melting of the binder phase during Grade C treatment the WC grains can easily be displaced, and a localized Co concentration is prevented due to the capillary forces of the liquid phase. As the characteristic discontinuities of Grade C there only remain coarse WC grains or their agglomerates (Fig. 3c). Having overall diameters of 10 to 12 μm they are present in all three grades of the material. The characteristic types of microstructural inhomogeneities must be kept in mind when the failure-initiating flaw size is discussed.

3.2. Mechanical strength data

Table II contains strength data of the three grades of the cemented carbide. The data represent mean values resulting from at least four individual measurements, except for the bend strength which was taken from a Weibull plot at 50% failure probability. This plot is shown in Fig. 4. It clearly demonstrates that the bend strength of Grades B and C is increased by a factor of about two compared to the as-sintered Grade A material. Even the scatter of the strength data is diminished in Grade C resulting in a steeper slope of the distribution curve and, hence, in an increased Weibull parameter. This result reflects the improved homogeneity of grade C where pores and Co pools are eliminated and just a small number of coarse WC agglomerates are still present.

Except for the bend strength, all mechanical strength parameters of Table II are nearly unaffected by the HIP treatment. This is particularly

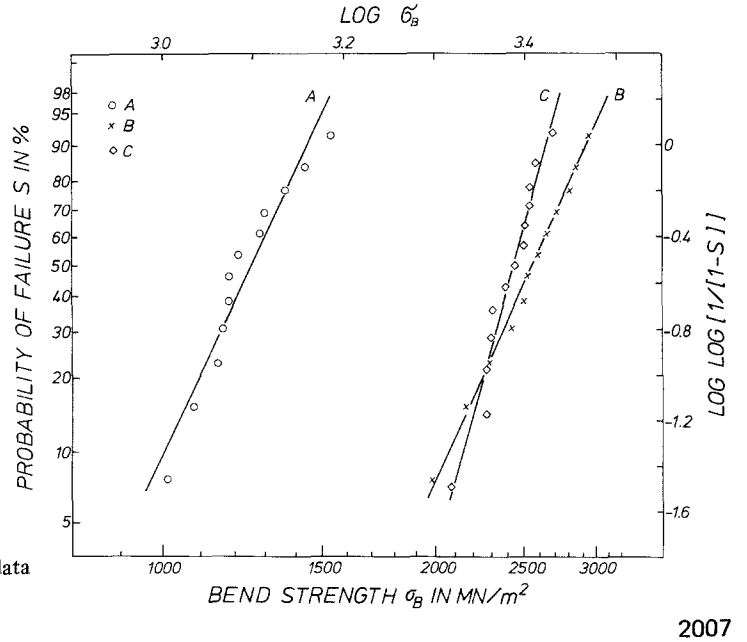

Figure 4 Distribution of bend strength data in a Weibull plot.

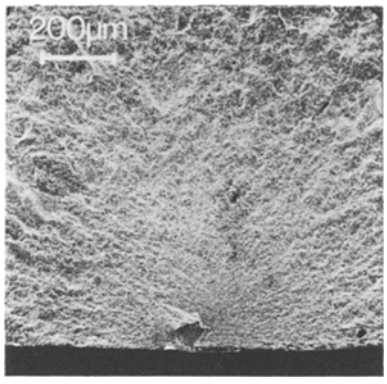

Figure 5 Fracture surface of a bend specimen. The fracture origin is located close to the lower specimen face. (SEM technique).

true of the specific work of fracture which has been shown previously to be strongly dependent on the composition and microstructural changes of cemented carbides [11]. Compared to the theoretical value of the thermodynamic surface energy of about $1\,J\,m^{-2}$, the experimental value of $70\,J\,m^{-2}$ demonstrates that an essential portion of the fracture energy is consumed by plastic deformation. The constancy of this parameter shows, however, that the amount of plasticity during fracture remains unchanged by HIP even on a microscopic scale.

A fairly good agreement can be observed between the two fracture energies γ_F and γ_I which are determined with completely different test methods. This result is not common in brittle material where, in general, a considerable dominance of γ_F over γ_I is found.

There is actually no change in the fracture toughness values due to the HIP treatment. The differences between Grades A to C are smaller than the experimental error limits. From the constancy of K_{IC} and γ_F it must be concluded that the inherent mechanical properties of both the carbide skeleton and the binder metal are not influenced by the HIP process.

3.3. Fractography

In SEM investigations of fracture surfaces, the origin of failure in the broken bend samples was localized. In Fig. 5 a fracture surface of a Grade A specimen is shown at a low magnification. From the diverging crack pattern it follows that the crack has started from the small inhomogeneity in the middle of the lower half of the micrograph beneath the lower sample surface.

It was found that in almost all cases the fracture-initiating flaws were located close to the sample face under tension, lying 10 to 80 µm beneath the surface. Three different types of fracture origins could be identified. The first kind of flaws are pores which were only observed in Grade A material. In the materials of Grade B and C, however, fracture starts from WC agglomerates and inclusions, respectively. Similar fracture origins have been reported [18–20]. In Fig. 6 an example is given of each type of flaw. Fig. 6a is a

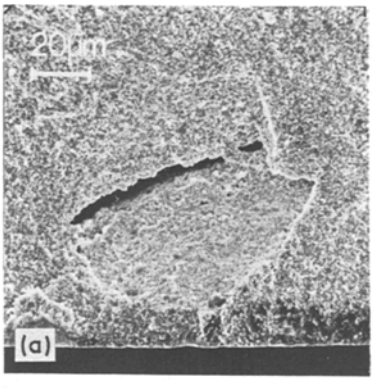

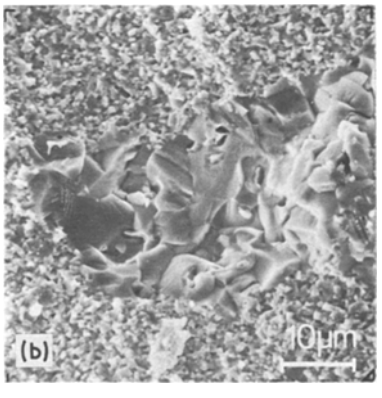

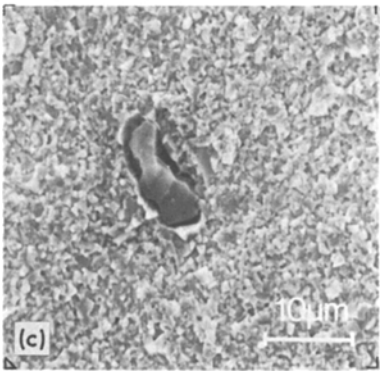

Figure 6 Different types of fracture origin; (a) pore (enlarged detail of Fig. 5), (b) agglomerate of coarse WC grains, and (c) inclusion. (SEM technique).

detail of Fig. 5 at a higher magnification showing a lens-shaped, flat pore as the fracture-initiating flaw. Its diameter with respect to the crack propagation direction is 45 μm. The failure origin shown in Fig. 6b is an agglomerate of coarse WC grains. The inclusion in Fig. 6 was analysed by EDAX techinque and found to consist mainly of Ca and S. These kinds of impurities are known to be already present in the raw material. From a series of SEM fracture micrographs the size of the fracture-initiating defects was determined quantitatively. In Section 4 these data are compared with theoretical flaw-size values.

4. Discussion

A study of the influence of HIP on the microscopic parameters and the macroscopic strength data reveals the following facts. The porosity of the material is reduced by 0.16% to almost zero. The metallographic analysis shows that the pores are completely eliminated in Grade B and C materials. Other microstructural parameters, however, remain unchanged ($\bar{D}_{WC}$, l_{Co}, C). The bend strength is increased by a factor of two, whereas all other mechanical properties are not affected at all (E, H_V 20, K_{IC}), or vary at best only very slightly (γ_F).

4.1. Proof of the Griffith theory in cemented carbides

The experimental data on both K_{IC} and γ_F indicate that the cemented carbide is a material which is nearly as brittle as ceramics. It seems to be justified, therefore, that the strength increase should be treated in terms of Griffith's theory. In this model the strength of a brittle material, as given by Equation 1 or 3, is governed by two material properties, i.e. an inherent strength parameter (K_{IC} or γ_I), and the flaw size, a. However, since K_{IC} is not increased by HIP the strength improvement should be caused by the change in flaw size only.

This approach could be proved to be true in two ways. Firstly the distribution of flaw sizes is considered. Knowing the value of the fracture toughness, the theoretical flaw size of each individual specimen which must have led to failure in the bend test can be calculated from the Griffith equation. This calculation was done using Equation 3 where a is the length of a surface crack or the half-length of an inside crack. Since fractographic examinations have shown that the fracture process always started from inside cracks Equation 3 can be written

$$a_{th} = \frac{2}{\pi}\left(\frac{K_{IC}}{\sigma_{eff}}\right)^2. \quad (7)$$

In Equation 7 σ_{eff} is the maximum local stress at the point where fracture starts. In three-point bending the stress decreases linearly along the sample axis, and σ_{eff} is given by

$$\sigma_{eff} = \sigma_B(1 - 2\Delta l/l) \quad (8)$$

where Δl is the distance between the fracture site and the centre line of the sample. Since fracture always originated very close to the lower specimen surface the stress decrease along the specimen height need not be considered.

Using Equations 7 and 8 a theoretical flaw size value is obtained for each data point of the Weibull plot, Fig. 4. This flaw-size distribution is shown in Fig. 7.

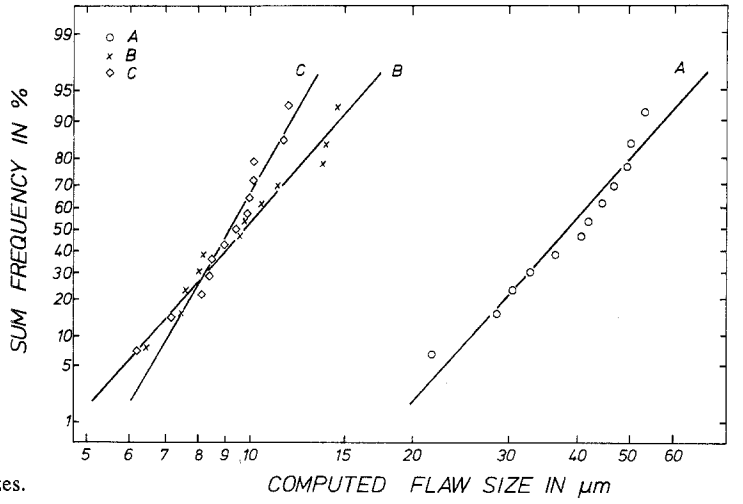

Figure 7 Distribution of computed flaw sizes.

The flaw sizes of the as-sintered material vary from 20 to 50 μm. In metallographic investigations (Section 3.1) pore diameters were found to lie in the same range of values. These pores can act as fracture origins as has been detected in fractographic examinations (Figs. 5 and 6a). In the densified materials, Grades B and C, pores do not exist to initiate failure. The theoretical flaw size is calculated to be about 6 to 14 μm (Fig. 7). Microstructural inhomogeneities in these grades, like coarse WC grains, inclusions, and Co pools, however, are of the same magnitude. Even though these particles do not represent real cracks they can act as stress concentrators in an otherwise homogeneous matrix. Since stress concentrations can cause sub-critical crack growth even at a low external stress, a crack may slowly grow along the boundary between the coarse particle and the matrix until the particle length is reached. If the stress is enhanced further the crack can act as a fracture-initiating flaw when the stress intensity factor at its tip attains the critical value of the surrounding matrix. Experimental evidence of an inclusion and a WC agglomerate that act in this sense has been given in Figs. 6b and 6c. Co pools could not be observed to initiate failure. It can be supposed, however, that the larger distribution of strength values of Grade B material compared to Grade C (Fig. 4) is caused by the additional presence of these defects. This interpretation is supported by the results of other authors [20].

The statistical treatment of bend strength values shows that there exists a strong quantitative equivalence between the flaw size calculated from the strength equation and the microstructural defects. In order to establish a second proof of the validity of Griffith's basic strength equation in cemented carbides a direct correlation of the fracture strength to the fracture-initiating flaw size was made. On a series of twelve broken specimens, the flaw size, a, with respect to the main crack propagation direction was determined fractographically and the respective local effective fracture stress was calculated from the experimental bend strength value using Equation 8. These data are plotted in Fig. 8 in a σ_{eff} versus $a^{-1/2}$ diagram. All data points lie very well on a straight line that goes through the origin of the plot, as predicted by Equation 3. The flaw sizes extend over one order of magnitude from 7 to 70 μm. Different symbols mark different microstructural fracture origins, the pores representing

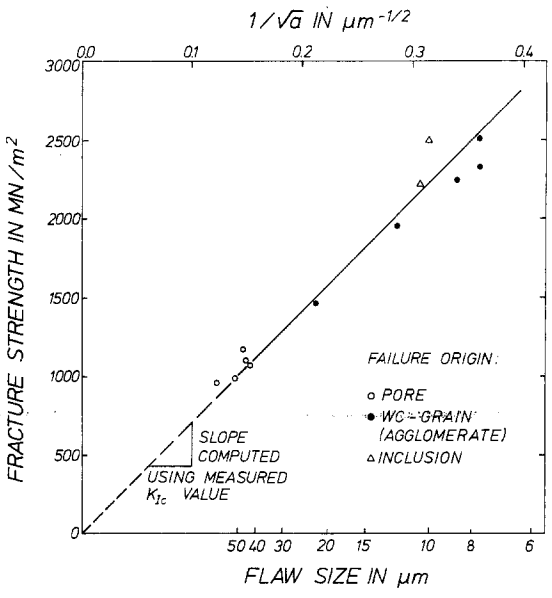

Figure 8 Dependence of local fracture stress on the flaw size.

the smallest strength data and the largest flaw-size values.

According to Equation 3, the slope of the σ_{eff} versus $a^{-1/2}$ plot is given by the K_{IC} value of the material in question. Taking K_{IC} from Table II, the slope was computed and inserted into Fig. 8 as the dashed and solid straight line. The good agreement between the theoretical line and the data points indicates that both the linear relationship and the correct numerical factor of Equation 3 are reproduced exactly. By this result the assumption that the strength of all three cemented carbide grades is controlled by the size of the fracture-initiating flaws is confirmed convincingly in terms of Griffith's theory.

4.2. Validity of K_{IC} results

The K_{IC} data reported in this work were obtained on samples that contained unusually deep cracks without measuring their length. For a quantitative interpretation of the strength properties in terms of Griffith's theory the correct numerical value of K_{IC} is of great importance. An erroneous K_{IC} measurement reveals data that usually are too large because the smallest value is always the correct one. The validity of the experimental determination of K_{IC} is discussed by means of three considerations; specimen dimensioning and plastic zone size, correspondence of γ_{F} and γ_{I}, and consistency of γ_{F} and the crack resistance curve $R(c)$.

The plastic zone size determines the minimum dimensions of the specimen. Its radius in plane strain is given by [21]

$$r_{pl} = \frac{1}{2\pi}\left(\frac{K_{IC}}{\sigma_Y}\right)^2. \quad (9)$$

Assuming for σ_Y a lower limit of 2000 MN m^{-2} [22], and inserting for K_{IC} the value found in this work, r_{pl} is about 3 μm. Thus, the conditions of plane strain fracture toughness testing are fully satisfied [23].

In basic fracture mechanics the specific fracture energy takes a single value. Hence, the ratio of the two quantities γ_F and γ_I should be equal to unity. In brittle ceramic materials, however, that ratio is found to be both greater (up to a factor of 4) and smaller than unity [24]. Values of $\gamma_F : \gamma_I > 1$ only occur in connection with an increasing R-curve and are indicative of an increasing energy consumption during fracture due to the enlargement of the process zone ahead of the crack tip, and a $\gamma_F : \gamma_I < 1$ relationship demonstrates that the value determined for K_{IC} (and hence γ_I) is too large, i.e. incorrect [24]. The ratio calculated from Table II varies from 1.17 to 1.29. Thus, γ_I seems to represent the true value of the material. Fracture mechanics postulates that the R curve of a brittle material should be a step function of the crack length having a constant R value that is twice the value of γ_F. It has been shown, however, that there are materials exhibiting an increasing R-curve where a unique K_{IC} parameter does not exist when these materials are pre-packed by slow crack growth [17]. Using the experimental technique reported by Kleinlein and Hübner [25] the R-curve of Grade A cemented carbide was determined experimentally. It is shown in Fig. 9. After a small increase within the first few per cent of crack growth the material is characterized by a nearly horizontal shape of the R-curve. Its numerical value of about 150 J m^{-2} is only slightly greater than twice the work of fracture, γ_F.

From the good consistency between the parameters γ_F, γ_I and R which are all determined with completely different experimental methods, the validity of the K_{IC} measurement is believed to be established.

5. Conclusions

It has been demonstrated in this work that the mechanical behaviour of the cemented carbide materials can be accurately described by basic fracture mechanics. The strength is controlled by the Griffith mechanism. Varying from Grade A to C, different microstructural defects act as the Griffith flaws, i.e. in Grade A, pores; in Grade B, Co pools, coarse WC grains, and inclusions; and in Grade C, coarse WC grains and inclusions.

The extent of the strength improvement achieved by HIP is limited by the size of the coarse WC grains and the inclusions. The pores still present after HIP do not control the strength any more.

On the basis of these results a further improvement in strength should be possible if microstrutural inhomogeneities can be eliminated further. The highest obtainable strength can be estimated from the Griffith equation if it is assumed that all major defects can be suppressed and that the grain size of the WC skeleton acts as the critical flaw size. This upper limit is about 7000 MN m^{-2}.

Considering the temperature dependence of the HIP process, a treatment at a temperature above the eutectic point is to be preferred. The smaller spread of the strength data of Grade C material is favourable with regard to technical application because the design of structural parts is not determined by the average strength but by a given probability of failure.

Acknowledgements

The authors wish to express their thanks to Professor O. Rüdiger, Friedr. Krupp GmbH, Forschungsinstitut, Essen, for the supply of the

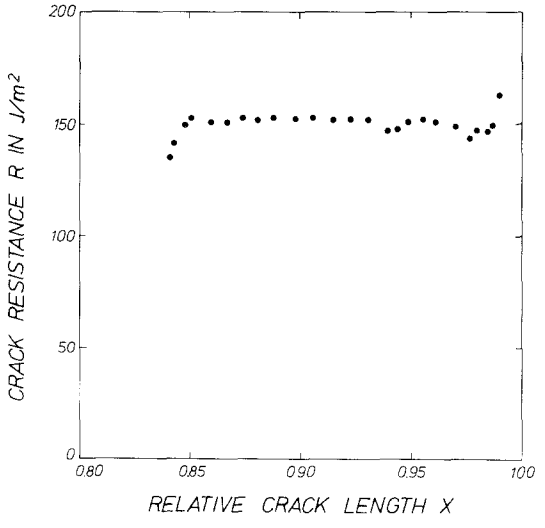

Figure 9 Crack resistance curve of Grade A material.

alloy and to Professor B. Ilschner for a critical reading of the manuscript.

References

1. P. B. ANDERSON, *Planseeber. Pulvermet.* **15** (1967) 180.
2. H. SUZUKI and K. HAYASHI, *ibid* **23** (1975) 24.
3. E. LARDNER and D. J. BETTLE, *Metals Mater.* 7 (1973) 540.
4. O. RÜDIGER and H. E. EXNER, *Powder Met. Int.* 8 (1976) 7.
5. R. W. DAVIDGE and A. G. EVANS, *Mater. Sci. Eng.* 6 (1970) 281.
6. P. KENNY, *Powder Met.* **14** (1971) 22.
7. N. INGELSTRÖM and H. NORDBERG, *Eng. Fracture Mech.* 6 (1974) 597.
8. W. DAWIHL, O. JUNG, and E. KOHLHAAS, *Arch. Eisenhüttenwes.* **45** (1974) 729.
9. J. L. CHERMANT and F. OSTERSTOCK, *J. Mater. Sci.* **11** (1976) 1939.
10. H. E. EXNER, A. WALTER, and R. PABST, *Mater. Sci. Eng.* **16** (1974) 231.
11. H. HÜBNER, *Z. Metallkde.* **67** (1976) 507.
12. H. HÜBNER and U. ENGEL, *Z. Werkstofftechnik* **9** (1978) 128.
13. H. E. EXNER, *Prakt. Metallog.* 3 (1966) 334.
14. *Idem, Metall.* **21** (1967) 431.
15. J. NAKAYAMA, *J. Amer. Ceram. Soc.* 48 (1965) 583.
16. H. G. TATTERSALL and G. TAPPIN, *J. Mater. Sci.* 1 (1966) 296.
17. H. HÜBNER and W. JILLEK, *ibid.* **12** (1977) 117.
18. E. ALMOND and R. ROEBUCK, *Powder Met.* **19** (1976) 109.
19. S. BARTOLUCCI-LUYCKX, *Acta Met.* **23** (1975) 109.
20. H. SUZUKI, T. TOMAE, and K. HAYASHI, *Planseeber. Pulvermet.* **23** (1975) 121.
21. G. R. IRVIN "Handbuch der Physik" Vol. VI (ed. S. Flügge) (Springer-Verlag, 1958).
22. J. BURBACH, *Techn. Mitt. Krupp, Forsch. Ber.* **26** (1968) 1.
23. W. F. BROWN and J. E. SRAWLEY, ASTM STP 410 (1966).
24. H. HUBNER and W. STROBL, *Ber. DKG* **54** (1977) 401.
25. F. W. KLEINLEIN and H. HÜBNER, Proc. ICF4, Waterloo 1977, Vol. 3, p. 883.

Received 22 December 1977 and accepted 20 January 1978.